Attractive Bridging Interactions in Dense Polymer Brushes in Good Solvent Measured by Atomic Force Microscopy

Diane Goodman,[†] Jayachandran N. Kizhakkedathu,[‡] and Donald E. Brooks*[,†,‡]

Department of Chemistry and Department of Pathology and Laboratory Medicine, University of British Columbia, Vancouver, British Columbia, V6T 2B5, Canada

Received October 2, 2003. In Final Form: January 9, 2004

Using an atomic force microscope (AFM), we have investigated the interaction forces exerted by latex particles bearing densely grafted polymer brushes consisting of poly(*N*,*N*-dimethylacrylamide) (PDMA), poly(methoxyethylacrylamide) (PMEA), poly(*N*-isopropylacrylamide) (PNIPAM), and PMEA-*b*-PNIPAM in aqueous media (good solvent). The brushes were prepared by controlled surface-initiated atom transfer radical polymerization, and the hydrodynamic thicknesses were measured by dynamic light scattering. The molecular weight (M_n), grafting density (σ), and polydispersity (PDI) of the brushes were determined by gel permeation chromatography and multiangle laser light scattering after cleaving the polymer from the latex surface by hydrolysis. Force profiles of PDMA (0.017 nm^{-2} ≤ σ ≤ 0.17 nm^{-2}) and PMEA (σ = 0.054 nm^{-2}) brushes were purely repulsive upon compression, with forces increasing with M_n and σ, as expected, due to excluded volume interactions. At a sufficiently low grafting density (σ = 0.012 nm^{-2}), PDMA exhibited a long-range exponentially increasing attractive force followed by repulsion upon further compression. The long-range attractive force is believed to be due to bridging between the free chain ends and the AFM tip. The PNIPAM brush exhibited a bridging force at a grafting density of 0.037 nm^{-2}, a value lower than the σ needed to induce bridging in the PDMA brush. Bridging was therefore found to depend on grafting density as well as on the nature of the monomer. The grafting densities of these polymers were larger than those typically associated with bridging. Bridging interactions were used to confirm the presence of PNIPAM in a block copolymer PMEA-*b*-PNIPAMA brush given that the original PMEA homopolymer brush produced a purely repulsive force. The attractive force was first detected in the block copolymer brush at a separation that increased with the length of the PNIPAM block.

Introduction

Terminally attached polymers having a distance between grafting points D less than twice their radius of gyration R_g are referred to as brushes and behave quite differently from their lower density ($D > 2R_g$) counterparts, known as mushrooms. In a good solvent, the polymer layer of a brush can be detected at a distance from the surface that is many times the R_g.[1] The polymer extends beyond R_g to avoid a loss in configurational entropy due to the high local segment density in the brush, despite the penalty incurred by chain stretching. Ultimately, there is a balance between these two effects, with the equilibrium structure reflecting the minimum global free energy state. Compression of the brush by a solid surface or by another brush increases the unfavorable segment overlap and gives rise to a repulsive entropic force. It is this repulsion that is responsible for the increased stability of colloids bearing end-grafted polymers.[2] The entropic repulsion of macromolecules such as proteins by brushes has led to their widespread application in materials for sensors or chemical gates,[3] drug delivery vehicles,[4] and chromatography media,[5] to name a few.

Compression of a brush by a solid particle or macromolecule has been investigated extensively from a theoretical perspective.[6−12] The reduction in entropy associated with increasing the local segment concentration in the region of confinement results in a repulsive force. Favorable contacts between a segment of the brush polymer and the interacting surface, however, lead to an attraction of the brush for the particle or free macromolecule, opposing the entropic repulsion required for effective protein exclusion. The overall interaction between a species and a brush layer depends, therefore, on a delicate balance between excluded volume effects and attractive interactions.

The surface force apparatus (SFA)[13−17] and atomic force microscope (AFM)[18−31] have been used over the past decade to directly measure the force exerted by end-grafted

* Corresponding author. Mailing address: Prof. Donald E. Brooks, 2211 Wesbrook Mall, Department of Pathology and Lab Medicine, University of British Columbia, Vancouver, BC, V6T 2B5, Canada. Phone: (604) 822-7081. Fax: (604) 822-7635. E-mail: don.brooks@ubc.ca.

[†] Department of Chemistry.

[‡] Department of Pathology and Laboratory Medicine.

(1) Israelachvili, J. N. *Intermolecular and Surface Forces*, 2nd ed.; Academic Press: London, 1992.

(2) Napper, D. H. *Steric Stabilization of Colloidal Dispersions*; Academic Press: London, 1983.

(3) Ito, Y.; Inaba, M.; Chung, D. J.; Imanishi, Y. *Macromolecules* **1992**, *25*, 7313.

(4) Woodle, M.; Lasic, D. *Biochim. Biophys. Acta* **1992**, *1113*, 171.

(5) Van Zanten, J. H. *Macromolecules* **1994**, *27*, 6797.

(6) de Gennes, P. G. *J. Phys.* **1976**, *37*, 1443.

(7) Alexander, S. *J. Phys.* **1977**, *38*, 983.

(8) Fleer, G. J.; Cohen-Stuart, M. A.; Scheutjens, J. M. H. M.; Cosgrove, T.; Vincent, B. *Polymers at Interfaces*; Chapman and Hall: London, 1993.

(9) Milner, S.; Witten, T.; Cates, M. *Macromolecules* **1988**, *21*, 2610.

(10) Wijmans, C. M.; Zhulina, E. B. *Macromolecules* **1993**, *26*, 7214.

(11) Johner, A.; Joanny, J.-F. *J. Chem. Phys.* **1992**, *96*, 6257.

(12) Tang, W. H.; Witten, T. A. *Macromolecules* **1996**, *29*, 4412.

(13) Raviv, U.; Frey, J.; Sak, R.; Laurar, P.; Tadmor, R.; Klein, J. *Langmuir* **2002**, *18*, 7482.

(14) Eiser, E.; Klein, J. *Phys. Rev. Lett.* **1999**, *82*, 5076.

(15) Sheth, S. R.; Efremova, N.; Leckband, D. E. *J. Phys. Chem. B* **2000**, *104*, 7652.

(16) Sheth, S. R.; Leckband, D. *Proc. Natl. Acad. Sci. U.S.A.* **1997**, *94*, 8399.

10.1021/la035843t CCC: $27.50
Published on Web 02/14/2004

polymer layers on a solid surface. Typically, a monotonically increasing repulsive force has been reported[15−17,20−31] which varies roughly exponentially with distance. In some cases, fits to the modified Alexander−de Gennes expression[32] derived for the force exerted by surfaces bearing polymer brushes in good solvent have given fit parameters for equilibrium thickness and grafting densities that agree reasonably well with those obtained from independent methods.[17,28]

Attraction between grafted polymer chains and a surface, which has been reported less frequently, is typically associated with systems in which the polymer can simultaneously adsorb onto two surfaces and pull them together.[33−44] The response of an elastic chain to the confinement of both ends is to reduce their separation, giving rise to the so-called bridging force.[1] Attractive segment−surface interactions as well as available adsorption sites on the surface are necessary for bridging to occur, with the optimum condition believed to be moderate surface coverage. At low coverage, the density of bridges will be very low, while at high coverage such as in a brush, the lack of available binding sites on the surface prevents the polymers from forming bridges.[38]

The interaction between two curved mica surfaces immersed in poly(ethylene oxide) (PEO) in an aqueous medium (good solvent) over time showed long-range attraction at low coverage (early incubation time) which was replaced by a purely repulsive force as adsorption of polymer to both surfaces approached saturation with time.[33]

Bridging is generally detected at low surface coverage of telechelic polymers, which have two adsorbing end groups,[14,19] but is absent when the polymer has only a single adsorbing end even at low coverage.[17] The results demonstrate the ability of end-grafted nonadsorbing chains to act as stabilizers where adsorbing polymers promote flocculation.

Braithwaite et al.[41] detected a small attractive force between two surfaces when a bare glass probe and a glass substrate with adsorbed PEO were brought together. The requirement of free adsorbing sites was demonstrated by the purely repulsive force measured upon bringing together the two surfaces after PEO had been allowed to adsorb onto both the glass probe and the substrate. The attractive force observed in the first case was smaller than that typically seen in the literature. This was attributed to the use of higher rates of approach allowing insufficient time for bridges to form.

Experimental evidence of bridging has generally been associated with adsorbed polymer where actual values for the amount of bound polymer are often unspecified and the bridging trends are correlated only with incubation times. The compression profiles of densely grafted polymer brushes reported to date have all been purely repulsive. In this work, we have measured the interaction between well-characterized spherical polymer brushes and a silicon nitride AFM tip in aqueous media. In some ways, examining grafting on a flat surface is more convenient, particularly in that the surface geometry is more easily modeled. The disadvantage of grafting onto flat surfaces is the small quantity of grafted material available for analysis by gel permeation chromatography (GPC). Due to the high surface area of the latex used here, a sufficient amount of material was available for analysis enabling the measured forces to be correlated with the molecular weight and grafting density of the polymer layer.

In some cases, we observed a long-range attraction, despite the reasonably high grafting densities and good solvent quality that, in previous studies, have produced only a repulsive force. The bridging was highly dependent on the grafting density and on the nature of the monomer, with the poly(*N*-isopropylacrylamide) (PNIPAM) surface exhibiting a much stronger attractive force than the poly(*N*,*N*-dimethylacrylamide) (PDMA) of similar σ. The results provide insight into the brush properties that are responsible for bridging interactions, allowing for improved control over colloid stability.

Experimental Section

Synthesis of Polymers Grafted from Atom Transfer Radical Polymerization (ATRP) Initiator Functionalized Latex. The synthesis of ATRP initiator functionalized latex has been described in a previous report in detail.[45] Briefly, narrowly dispersed polystyrene (PS) seed latex was synthesized by surfactant-free polymerization of styrene in water initiated by potassium persulfate (KPS) at 70 °C for 24 h under an argon atmosphere. A copolymer shell of styrene and ATRP initiator monomer 2-(methyl 2′-chloropropionato)ethyl acrylate (HEA-Cl) was added to the PS seed latex by a shell growth polymerization. The hydrodynamic diameter of the shell latex was 650 nm for the PDMA brushes and 585 nm for the PNIPAM brushes. We followed the general methods reported in our earlier communications for the polymerization of *N*,*N*-dimethylacrylamide (DMA),[45] *N*-isopropylacrylamide (NIPAM),[46] and copolymerization of methoxyethylacrylamide (MEA)/NIPAM[47] on ATRP functionalized latex.

(17) Tauton, H. J.; Toprakcioglu, C.; Fetters, L. J.; Klein, J. *Macromolecules* **1990**, *23*, 571.
(18) Hartley, P. G.; McArthur, S. L.; McLean, K.; Griesser, H. J. *Langmuir* **2002**, *18*, 2483.
(19) Courvoisier, A.; Isel, F.; Francois, J.; Maaloum, M. *Langmuir* **1998**, *14*, 3727.
(20) Yamamoto, S.; Tsujii, Y.; Fukuda, T. *Macromolecules* **2000**, *33*, 5995.
(21) Kelley, T. W.; Schorr, P. A.; Johnson, K. D.; Tirell, M.; Frisbie, C. D. *Macromolecules* **1998**, *31*, 4297.
(22) Yamamoto, S.; Ejaz, M.; Tsujii, Y.; Matsumoto, M.; Fukuda, T. *Macromolecules* **2000**, *33*, 5602.
(23) Yamamoto, S.; Ejaz, M.; Tsujii, Y.; Fukuda, T. *Macromolecules* **2000**, *33*, 5608.
(24) Prescott, S. W.; Fellows, C. M.; Considine, R. F.; Drummond, C. J.; Gilbert, R. G. *Polymer* **2002**, *43*, 3191.
(25) Vermette, P.; Meagher, L. *Langmuir* **2002**, *18*, 10137.
(26) Kidoaki, S.; Ohya, S.; Nakayama, Y.; Matsuda, T. *Langmuir* **2001**, *17*, 2402.
(27) Kidoaki, S.; Nakayama, Y.; Matsuda, T. *Langmuir* **2001**, *17*, 1080.
(28) Butt, H.-J.; Kappl, M.; Mueller, H.; Raiteri, R. *Langmuir* **1999**, *15*, 2559.
(29) Overney, R. M.; Leta, D. P.; Pictroski, C. F.; Rafailovich, M. H.; Liu, Y.; Quinn, J.; Sokolov, J.; Eisenberg, A.; Overney, G. *Phys. Rev. Lett.* **1996**, *76*, 1272.
(30) Roters, A.; Schimmel, M.; Ruhe, J.; Johannsmann, D. *Langmuir* **1998**, *14*, 3999.
(31) O'Shea, S. J.; Welland, M. E.; Rayment, T. *Langmuir* **1993**, *9*, 1826.
(32) de Gennes, P. G. *Macromolecules* **1980**, *13*, 1069.
(33) Klein, J.; Luckham, P. F. *Nature* **1984**, *308*, 836.
(34) Israelachvili, J. N.; Tirrell, M.; Klein, J.; Almog, Y. *Macromolecules* **1984**, *17*, 204.
(35) Luckham, P. F.; Klein, J. *Macromolecules* **1985**, *18*, 721.
(36) Ingersent, K.; Klein, J.; Pincus, P. *Macromolecules* **1986**, *19*, 1374.
(37) Hu, H. W.; Van Alsten, J.; Granick, S. *Langmuir* **1989**, *5*, 270.
(38) Ji, H.; Hone, D.; Pincus, P. A.; Rossi, G. *Macromolecules* **1990**, *23*, 698.
(39) Ingersent, K.; Klein, J.; Pincus, P. *Macromolecules* **1990**, *23*, 548.
(40) Biggs, S. *Langmuir* **1995**, *11*, 156.
(41) Braithwaite, G. J. C.; Howe, A.; Luckham, P. F. *Langmuir* **1996**, *12*, 4224.
(42) Meagher, L.; Maurdev, G.; Gee, M. L. *Langmuir* **2002**, *18*, 2649.
(43) Muir, I.; Meagher, L.; Gee, M. *Langmuir* **2001**, *17*, 4932.
(44) Maurdev, G.; Meagher, L.; Ennis, J.; Gee, M. L. *Macromolecules* **2001**, *34*, 4151.
(45) Jayachandran, K. N.; Takacs-Cox, A.; Brooks, D. E. *Macromolecules* **2002**, *35*, 4247.
(46) Kizhakkedathu, J. N.; Norris-Jones, R.; Brooks, D. E. *Macromolecules*, in press.

Table 1. Properties of PDMA Brushes with $M_n \sim 30\,600$ and PDI = 1.35

time[a] (h)	σ[b] (nm^{-2})	D/R_g[c]	HT[d] (nm)	L_e[e] (nm)	L_e*[f] (nm)	a[g] (nN)	b[h] (nm^{-1})
0	0.17	0.38	58	65	65	1.0 ± 0.3	0.09 ± 0.02
1	0.081	0.55	40	48	48	0.8 ± 0.2	0.16 ± 0.02
5	0.038	0.80	30	34	34	0.3 ± 0.5	0.17 ± 0.06
7	0.031	0.87	40	32	32	0.4 ± 0.4	0.48 ± 0.01
15	0.022	1.0	32	25	15	0.6 ± 0.5	0.29 ± 0.04
24	0.017	1.2	42	15	10	0.3 ± 0.4	0.36 ± 0.05
48	0.012	1.4	49				

[a] Length of time the chains were hydrolyzed from the grafting surface. [b] Grafting density at the surface (chains/nm^2). [c] Ratio of the distance between grafting points to the radius of gyration. [d] Hydrodynamic thickness measured by the particle size analyzer. [e] Equilibrium thickness measured from force profiles before electrostatic correction. [f] Equilibrium thickness measured from force profiles after electrostatic correction. [g] Fitting parameter in eq 1 (see Figure 2). [h] Fitting parameter in eq 1 (see Figure 2).

Characterization of Grafted Latex. The grafted latex was characterized by determining hydrodynamic size, graft molecular weight, molecular weight distribution, and radius of gyration of polymer chains. Molecular weights were determined by GPC on a Waters 2690 separation module fitted with a DAWN EOS multiangle laser light scattering (MALLS) detector from Wyatt Technology Corp. with 18 detectors placed at different angles (laser wavelength $\lambda = 690$ nm) and a refractive index detector from Viscotek Corp. operated at $\lambda = 620$ nm. Nuclear magnetic resonance (NMR) was performed on a Brucker Avance 300 NMR spectrometer using deuterated solvents ($CDCl_3$, Cambridge Isotope Laboratories, 99.8% D) with the solvent peak as a reference. A detailed description of the methods is given in our earlier report.[45]

Particle size measurements (i.e., measurements of the hydrodynamic diameter distribution of particle suspensions) were carried out in a temperature-controlled Beckman Coulter N4 Plus particle size analyzer by dynamic light scattering. Aqueous dispersions of particles were allowed to thermally equilibrate for 5 min, and the measurements were made at 20 °C unless otherwise mentioned. Size analyses were performed using the software supplied by the manufacturer.

Preparation of PDMA Grafted Latex with Different Grafting Densities. The amount of polymer grafted was determined by quantitative release of the chains at the point of grafting by hydrolysis. The grafting density was calculated from the surface area of the latex and the amount and molecular weight of the polymer grafted as described previously.[45] Brushes with varying graft density and constant M_n were prepared by time-dependent quantitative hydrolysis of grafted PDMA latex. Grafted latex samples (4 g each) were stirred with NaOH (2 g, 2 N) for different periods of time (up to 96 h), and the hydrolysis was stopped by the addition of dilute (6 N) HCl to the suspension. The supernatant was collected quantitatively by centrifugation of the suspension. The graft densities of these cleaved brushes were determined from the amount of polymer released from different samples at various time intervals (Table 1).

AFM Measurements. Measurements were performed on a Multimode, Nanoscope IIIa controller (Digital Instruments (DI), Santa Barbara, CA), equipped with a fluid cell. Cantilevers were V-shaped silicon nitride with a tip radius of 5−40 nm and a spring constant of 0.06 N/m as quoted by the manufacturer (DI). The rate of tip−sample approach was typically 500 nm/s. Samples were prepared by drying the latex suspension onto a glass substrate (precleaned in chromic acid), followed by sonication and thorough rinsing with water to remove any latex which had not been strongly physisorbed. To minimize lateral motion during the force measurements, our goal was to prepare a closely packed monolayer of latex. Inspection under an optical microscope suggested regions of monolayer coverage were present. Force measurements were made in these regions.

Experiments were performed in a 10 mM NaCl solution, pH adjusted to 7.0 with dilute sodium bicarbonate solution. Since the structure of PNIPAM is known to be sensitive to salt concentration,[48] force measurements as a function of ionic strength were performed to confirm that in 10 mM NaCl the polymer was in an extended conformation. Samples were allowed to equilibrate for 15 min before performing experiments.

The inaccuracy of the spring constant quoted by the manufacturer does not allow for direct comparison of results obtained using different tips; therefore a single tip was used to probe the poly(methoxyethylacrylamide) (PMEA), PNIPAM, and copolymer samples. The force between the tip and a clean glass substrate was measured before and after probing each sample to check tip quality. A consistent profile was observed with only a snap-to-contact attraction at very small separations and a primary adhesive force upon retraction, suggesting that the tip remained free of contaminants. By comparison, we have seen that when the tip is contaminated by adsorbed polymer, the retraction profile of the tip on a clean glass surface exhibits an attractive force that varies nonlinearly with extension that is characteristic of the stretching of polymer chains. Such behavior was not observed during our routine tests of tip quality where force profiles on clean glass substrates were obtained. The integrity of the data was further verified by repeating the measurements with different tips and freshly prepared samples; we found that the results were qualitatively the same. Due to the inaccuracy of the spring constant, we did not compare the results quantitatively. The tips were also inspected under an optical microscope following measurements to ensure that contamination by large particles such as latex had not occurred.

Force measurements were repeated at various locations on each sample. In cases where pure repulsion was observed, the profiles were very reproducible, suggesting that effects from curvature of the latex did not contribute significantly to the measurements.

Data Analysis. The optical sensitivity (V/nm) was calibrated on a hard glass surface by measuring the slope of the linear region of the raw force curve (photodiode (V) vs piezo position (nm)) after contact had been made with the glass. The cantilever deflection (nm) is obtained by dividing the measured photodiode signal (V) by the optical sensitivity. On a hard surface, the change in cantilever deflection (Δd) is equal to the change in piezo or sample position (Δh). The laser and cantilever were not adjusted after calibration, enabling the same optical sensitivity to be used on the grafted polymer samples. Forces were calculated from the measured cantilever deflection by multiplying Δd by the cantilever spring constant according to Hooke's law.

Tip−sample separations (Δz) were obtained by subtracting the change in tip deflection from the measured relative sample position according to the method of Ducker et al.[49] Separation $z = 0$ corresponded to the position at which the sample behaved as a hard surface upon further compression, commonly known as the constant compliance regime. It is often difficult to fully compress polymer brushes using a cantilever of a given stiffness, particularly when the grafting density is very high. All of the brush samples used here could be compressed to the point where the slope ($\Delta d/\Delta h$) of the deflection versus position curve was equal to 1, the same as that of the glass substrate.

To give some physical meaning to the separations, we have assumed that $z = 0$ corresponds to the point where the tip nearly contacts the latex surface. It is of course possible that the polymer cannot be further compressed and behaves like a hard surface while a significant, incompressible layer of polymer remains between the tip and the latex. This has been referred to by other authors[20] as an offset distance. There, the offset distance in a brush of $\sigma = 0.07$ nm^{-2} was determined by scanning across the boundary of the polymer sample and a bare patch of substrate where the polymer was removed. They found an offset distance of 14 nm when measurements were obtained with a silica probe (10 μm diameter) but an offset distance of zero when using a standard V-shaped cantilever of the type used here. They attributed this to the ability of the sharp tip to penetrate the

(47) Kizhakkedathu, J. N.; Kumar, K. R.; Goodman, D.; Brooks, D. E. *Macromolecules*, submitted.

(48) Park, T. G.; Hoffman, A. S. *Macromolecules* **1993**, *26*, 5045.

(49) Ducker, W. A.; Senden, T. J.; Pashley, R. M. *Langmuir* **1992**, *8*, 1831.

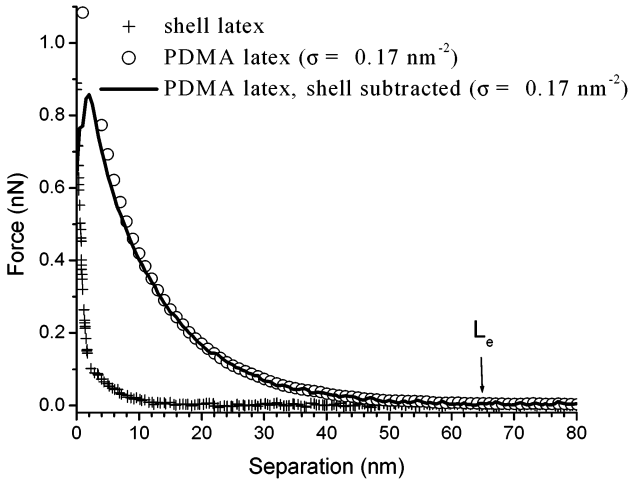

Figure 1. Compression profile of PDMA brushes ($M_n = 30\,600$) grafted to polystyrene latex particles (650 nm diameter) before and after correction for the electrostatic contribution. The purely electrostatic profile of the shell latex is also shown. AFM measurements were performed in 10 mM NaCl. The shell and brush profiles are averages of 10 and 75 curves, respectively. The arrow denotes the separation corresponding to the equilibrium brush thickness, L_e.

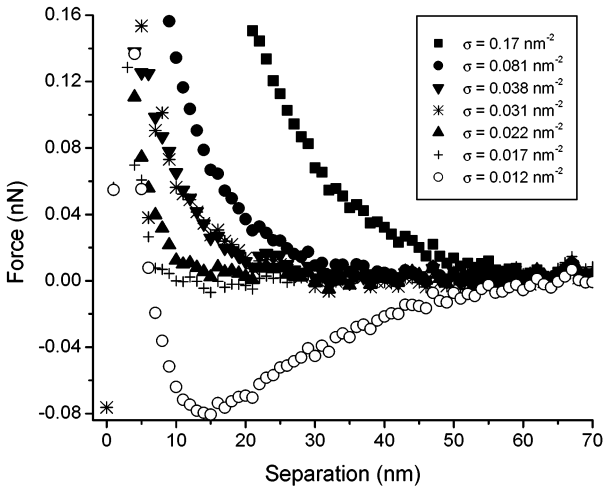

Figure 2. Effect of grafting density on compression of PDMA brushes ($M_n = 30\,600$) grafted to polystyrene latex particles measured in 10 mM NaCl. Curves have been corrected to remove the electrostatic contribution (see the text). Each curve represents the average of data from ~75 locations on the sample. See the text and Table 1 for a discussion of uncertainty.

polymer layer and closely approach the substrate. While we did not measure the offset distance, we believe that our approximation of zero offset is reasonable given our use of sharp Si_3N_4 probes and grafting densities generally lower than or near that in the referenced report,[20] except for the highest σ PDMA brush.

Force measurements on the nongrafted shell latex showed that at this ionic strength, repulsion between the negatively charged tip and latex occurred over a relatively small separation range and magnitude. In some low grafting density cases, this contribution was non-negligible. The force profiles obtained on the shell latex were subtracted from the PDMA brush profiles (refer to results section) to remove the electrostatic contribution and to allow the steric brush forces to be examined independently. This approach seems reasonable since the charge density is not affected by the grafting reaction.

The equilibrium thickness of the brush was taken as the separation at which tip deflection first deviated significantly from the baseline, corresponding to a repulsion of ~0.02 nN.

Results and Discussion

The results are summarized in four sections. We first present the effect of grafting density on the relative bridging (attractive) and excluded volume (repulsive) contributions to the force profile of a PDMA brush. We then compare brushes prepared from PDMA and PNIPAM having similar M_n and σ to examine the effect of changing the nature of the monomer. In the third section, we present the results for a series of PMEA-*b*-PNIPAM copolymers with the same length PMEA block (same σ) and increasing PNIPAM block length. Finally, we compare the adhesion of the bridged and nonbridged chains to the tip measured by pulling on the compressed brush in the direction away from the grafting surface.

Effect of Grafting Density. Surfaces having the same M_n and different σ were obtained by hydrolyzing the highest σ brush for various lengths of time and thereby cleaving different number fractions of the chains at their point of grafting. The brush properties are listed in Table 1.

Force profiles were obtained upon compressing the PDMA brush samples of varying σ as well as the nongrafted shell latex in 10 mM NaCl. The force profile of the negatively charged shell latex shown in Figure 1 is electrostatic in nature and results from the osmotic repulsion of the double-layer counterions. The curve shown is an average of 10 force profiles obtained over the latex surface. The data corresponding to separations of >1.5 nm fit an exponential with a measured decay length of 3.37 ± 0.09 nm which compares with the Debye length of 2.88 nm.[1] The compression profile of the PDMA brush having the highest grafting density ($\sigma = 0.17$ nm^{-2}) is also presented in Figure 1. The curve is an average of 75 force profiles obtained over the sample surface. At large separations, the repulsive force is due mainly to the steric interaction from the grafted layer. At smaller separations, both steric and electrostatic forces contribute to the profile. The effect of the grafted layer can be examined independent of electrostatics by subtracting the shell profile from the brush profile, as indicated by the solid line. As demonstrated by the superposition of the brush profiles before and after shell subtraction at small loads (<0.35 nN), the force profile of the $\sigma = 0.17$ nm^{-2} brush is not significantly affected by the underlying shell latex interactions at long range. The same value for the equilibrium thickness ($L_e = 65$ nm), corresponding to the first detectable repulsive interaction, is obtained when taken from either the nonadjusted or corrected curve in Figure 1. This is true for all samples with σ between 0.031 and 0.17 nm^{-2}. When the grafting density is lowered to 0.022 nm^{-2}, the range of separation and magnitude of the steric force are sufficiently decreased that the electrostatic interactions become significant at smaller loads. In these cases, different values are obtained for the equilibrium thickness when measured before and after the electrostatic correction. Both values are listed in Table 1.

The effect of varying σ on the compression force profile for PDMA is shown in Figure 2. The curves have all been corrected by subtracting the electrostatic contribution from the shell latex, as described above. The force profiles $F(z)$ presented for the PDMA brushes of varying grafting densities are the averages of curves obtained at ~75 different locations on each sample. The curves could be fit to a single increasing exponential:

$$F(z) = -ae^{-bz} \qquad (1)$$

where a and b are the fitting parameters (Table 1). We also calculated an upper bound curve from the mean plus

one standard deviation of each point and fit the curve to eq 1. The uncertainties for a and b given in Table 1 are calculated from the difference between the fit parameters obtained for the mean curve and the upper bound curve.

The separation at which deviation of the force from the baseline is first observed increases with σ. The more extended brush structure associated with larger σ is consistent with the stretching of the chains away from the grafting surface in response to the increased excluded volume.[8] The measured equilibrium thickness values are similar to the hydrodynamic thickness (HT) measurements obtained using the particle size analyzer as shown in Table 1. We present the HT values for comparison but recognize that propagation of the errors associated with the diameter estimates of the grafted and shell latexes gives rise to a large absolute uncertainty for relatively small HT values. The equilibrium thickness for the $\sigma = 0.012$ nm^{-2} brush, for which the force profile exhibited a long-range attraction, cannot be determined by this method. As discussed below in the section Relaxation of Bridged Chains, the attractive bridging interactions depend on the rate of the measurement and are therefore not equilibrium values.

When the grafting density is lowered to $\sigma = 0.012$ nm^{-2}, which, from D/R_g of ~1.4, corresponds to a moderately dense brush, long-range attraction is observed at a separation of 70 nm (Figure 2). It is here where the tip first contacts the outer layer of the brush and, with repulsion due to segment overlap minimal, the attractive bridging force is detectable. A repulsive force dominates upon further compression as the chains become increasingly confined.

It is believed that bridging is mainly due to the adsorption of tails. This is based on the analogy with self-consistent mean field calculations[8] of the relative amounts of trains, loops, tails, and bridges of an adsorbed polymer as a function of surface separation, which have predicted a reduction in tails with increased bridging upon compression and a roughly constant fraction of trains and loops. The detection of bridging by brushes with surface coverages higher than those generally reported may give information about the location of chain ends in the grafted polymer layer. If the free chain ends of the grafted polymer are buried within the random coil and are inaccessible to the penetrating species, entropic repulsion may dominate even at low grafting densities, as was noted in earlier studies.[17]

Numerous theoretical models have been developed to predict the distribution of chain ends in planar grafted polymer layers. In the model of Alexander and de Gennes,[6,7] a steplike concentration profile is assumed where all chain ends are found on the outer edge of the brush. More sophisticated approaches, however, predict a roughly parabolic concentration profile with chain ends distributed throughout the layer.[9] The total polymer concentration profile and the distribution of chain ends are functions of solvent quality and polydispersity.

An extension of these models to brushes on curved surfaces predicts a more dilute concentration profile and a so-called "dead zone", or absence of end segments in the region of the grafting surface.[10] Our spherical brushes, having a ratio of $R/(R + \mathrm{HT})$ between 0.92 and 0.97, where R is the radius of curvature of the latex particle, likely have a high fraction of accessible chain ends located away from the grafting surface, which favors the formation of bridges. The polymer volume fraction at the equilibrium thickness of our spherical brushes is also less than would be predicted for a flat surface of similar grafting density, somewhat reducing excluded volume effects so that the attractive bridging force can be observed. As the grafting density is further increased ($\sigma > 0.022$ nm^2), the excluded volume becomes too large and the repulsive force dominates. Despite the curvature effect, which is more pronounced when the ratio of HT to particle radius is large, the layers are still in the brush regime at all locations away from the grafting surface, with D^*/R_g ranging between 0.45 and 1.39, where D^* is the distance between chains calculated at the equilibrium thickness.

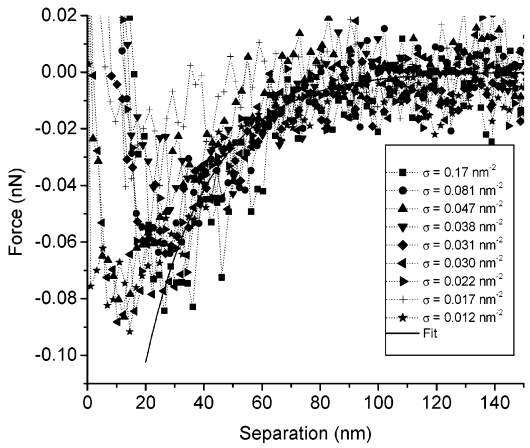

Figure 3. Long-range attraction in PDMA brushes at various grafting densities. Curves represent single force measurements where the infrequent occurrence of bridging was observed. Curves are fit to an increasing exponential.

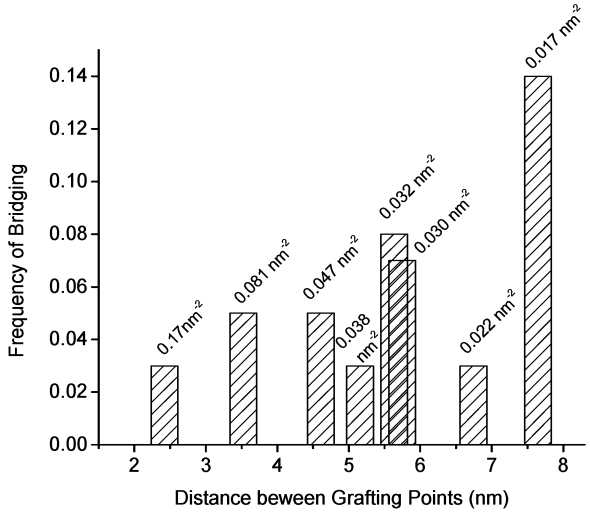

Figure 4. Frequency of bridging events ($N \sim 75$ measurements) observed in PDMA brushes of varying grafting density.

The profiles in Figure 2 are the average of force curves taken at over 75 different locations on a sample. In examining the individual data, however, we detect bridging even on the high σ samples, at a low sampling frequency (~3−14%). The individual profiles in which attraction was observed at various σ are presented in Figure 3. The frequency at which these bridging events was observed is shown in Figure 4. Due to the superposition of the curves at long range before and after the electrostatic correction, the data for the remainder of the report are left uncorrected, as the results presented are not significantly affected.

The anomalous bridging at high σ could in principle be the result of lateral inhomogeneities in the grafting (i.e., patches of low σ), where a decrease in local excluded volume would allow for attractive bridging to be observed. This interpretation seems unlikely, however, given that our

calculations have predicted a random distribution of initiator (HEA-Cl) over the surface.[45] Taking the number of moles of styrene and HEA-Cl used in the shell copolymerization and the reactivity ratios of styrene and *n*-butyl acrylate, a comonomer structurally related to our initiator at 60 °C,[50] we have used the microstructure equation[51] to calculate the probable distribution of initiator in the copolymer. We have found the diad and triad probabilities of the acrylate to be 6.1% and 0.4%, with diad, triad, and tetrad probabilities of styrene being 33%, 21%, and 1.4%, respectively. The distribution of the initiator throughout the copolymer is therefore very likely random.

An alternative explanation is that the tip infrequently samples long chains that extend well beyond the average equilibrium thickness into a region where the polymer fraction is low. It is known from GPC/MALLS that the sample contains a fraction of chains longer than the mean, due to the slight polydispersity (PDI = 1.35) that would be present in all samples. Since the long-range attractive regions for all values of σ may be fit to a single curve, the latter interpretation seems more plausible.

The data obtained by stretching the PDMA chains away from the grafting surface following compression, which are presented in another report,[52] support the above conclusion. The length of the stretched bridged chain, based on the separation corresponding to final rupture from the tip, was always larger than the calculated average contour length of 77 nm, which was estimated from the average degree of polymerization ($N = 309$ based on M_n) and the projected tetrahedral C−C bond length (0.25 nm). Final rupture for these anomalous profiles also occurred at separations greater than the average rupture separation measured when bridging was not detected upon compression. This suggests that the long-range attraction observed on compression is the result of bridging of above average length chains.

There has been theoretical and experimental research suggesting bridging decays roughly exponentially with distance,[34,38] the dependence being correlated with the exponentially decaying tail of the segment-density distribution near an adsorbing wall. While the volume fraction profile of end-grafted polymer away from a surface differs from that of adsorbed polymer, the data in Figure 3 fit an exponential decay. The decay length was found to be 22 ± 6 nm, which is significantly larger than the value of R_g (6.4 nm).

Effect of Monomer Type. The force profiles of PDMA and PNIPAM brushes having the same grafting density $\sigma = 0.038$ nm^{-2}, similar M_n (30 600 and 48 000), and D/R_g of 0.80 and 0.66, respectively, are compared in Figure 5. The electrostatic contributions have been subtracted. At this grafting density, the PDMA brush is repulsive at all separations whereas the PNIPAM brush exhibits a long-range attractive force which is followed by repulsion only at very small separations (~5 nm). Based on the measured hydrodynamic thickness of the PDMA (30 nm) and PNIPAM (100 nm) samples, we infer that both brushes are in an extended structure due to excluded volume effects. The ability of PNIPAM to bridge the AFM tip at higher σ than PDMA may reflect differences in the adsorption of the polymers to Si_3N_4 or differences in their excluded volume at a particular σ. The results imply that, depending on the monomer, significantly different grafting densities can be required to achieve the same entropic repulsion of brushes in good solvent.

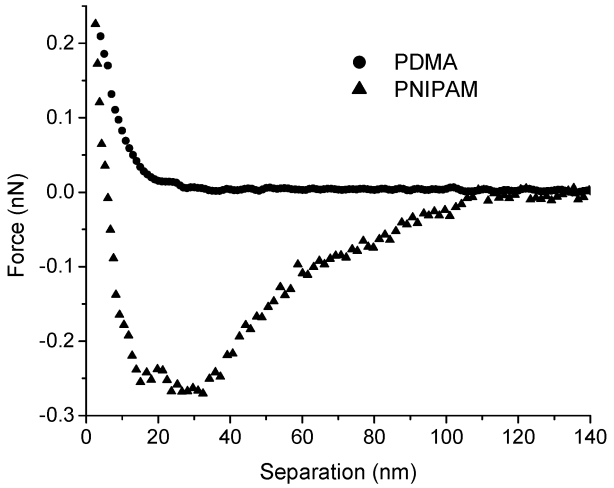

Figure 5. Effect of monomer type on compression of brushes. Curves show typical single force profiles. PDMA: $M_n \sim 30\,600$, $D = 5.1$ nm. PNIPAM: $M_n = 48\,000$, $D = 5.2$ nm. Measurements are in 10 mM NaCl, pH 7.

Table 2. Properties of PMEA-*b*-PNIPAM Copolymer Brushes[a]

$M_{n,PNIPAM}$	HT (nm)	L_A (nm)	$M_{n,PNIPAM}$	HT (nm)	L_A (nm)
0	17		42 500	72	105
9 700	40		93 500	153	142

[a] $M_{n,PMEA} = 32\,500$, $\sigma = 0.054$ nm^{-2}, PDI = 1.12.

Effect of Copolymer Block Length. The brush properties of the grafted copolymer layers having the first block consisting of PMEA of $M_n \sim 32\,500$, PDI = 1.24, and $\sigma = 0.054$ nm^2 and the second block of PNIPAM of variable M_n are listed in Table 2. The M_n of the PMEA homopolymer brush was determined by GPC/MALLS, while that of the copolymer brush was calculated from ^{1}H NMR compositions and the M_n of the first (PMEA) block.[47] We use NMR to characterize the brushes due to the difficulty in determining molecular weights of copolymers by GPC, as demonstrated in the literature.[53,54] It has been reported that the heterogeneity in the chemical composition of the copolymer affects the values of the refractive index increments along the chromatogram, resulting in inaccurate molecular weight determination.[53,54]

The force profiles of the homopolymer PMEA brush and the PMEA-*b*-PNIPAM copolymer brushes are presented in Figure 6. The PMEA homopolymer and the copolymer with the shortest PNIPAM block are repulsive at all separations and are indistinguishable. As the PNIPAM block length is increased, the force profiles exhibit a long-range attraction, where the onset of attraction, L_A, increases with PNIPAM block length (Table 2). The distinctly different profiles obtained before and after addition of the PNIPAM block make the preferential adsorption of PNIPAM to Si_3N_4 an easy way of confirming the presence of the second block. Although the presence of the shortest PNIPAM block could not be detected under these conditions, additional experiments in which a 10 μm polystyrene latex particle probe was used in place of the Si_3N_4 AFM tip gave rise to a strong long-range attraction to copolymers of all three PNIPAM block

(50) *Polymer Handbook*; Brandup, J., Immergut, E. H., Eds.; John Wiley & Sons: New York, 1989.
(51) Odian, G. *Principles of Polymerization*, 3rd ed.; John Wiley & Sons: New York, 1991; Chapter 6.
(52) Goodman, D.; Kizhakkedathu, J. N.; Brooks, D. E. *Langmuir*, submitted.
(53) Se, K.; Sakakibara, T.; Ogawa, E. *Polymer* **2002**, *43*, 5447.
(54) Radke, W.; Simon, P. F. W.; Muller, A. H. E. *Macromolecules* **1996**, *29*, 4926.

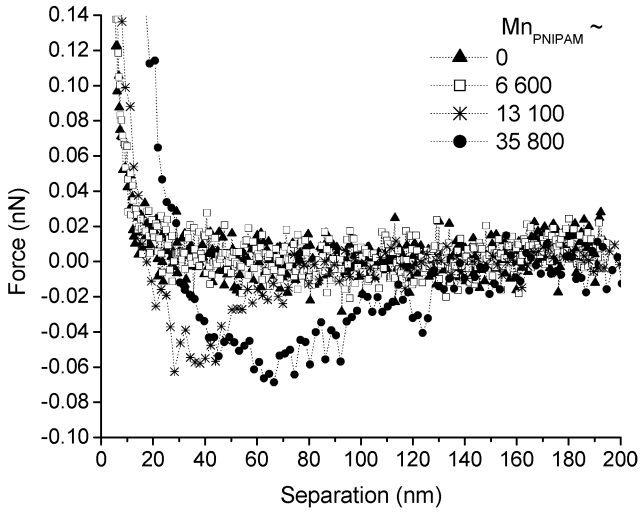

Figure 6. Effect of PNIPAM block length on compression of PMEA-*b*-PNIPAM copolymer brushes. Curves show typical single force profiles. PMEA: $M_n \sim 32\,500$, PDI = 1.12, $\sigma = 0.054$ nm^2. Measurements were performed in 10 mM NaCl, pH 7.

lengths.[47] The larger contact area increased the overall measured force and enabled detection of the bridging interaction of the shortest PNIPAM block, which was too weak to be detected with the Si_3N_4 probe.

Relaxation of Bridged Chains. The decompression profiles of brushes that have exhibited a long-range attractive force on approach show considerable hysteresis from the compression profiles. In Figure 7a, we present the results for the PMEA brush obtained in both advancing and receding directions. The absence of hysteresis indicates that at the rate of a compression/decompression cycle applied (500 nm/s), the compressed chains have returned to their equilibrium position at each separation. Furthermore, we repeated the measurements at various rates (100−3000 nm/s) and found no detectable dependence on the scan rate within the range tested when purely repulsive forces were observed.

In contrast, the decompression force of the PNIPAM brush in Figure 7b shows significant hysteresis and is much lower than the compression force at any given separation. Slow relaxation of chains relative to experimental decompression rates has been found to be characteristic of bridged polymers.[55] This gives rise to the hysteresis observed at small separations, in the region that corresponds to the beginning of decompression. For adsorbed polymers, this effect has been attributed to the temporarily higher fraction of polymer on the surface after compression, which reduces the mean concentration of polymer within the gap, resulting in a lower force.[35] In our case, where the chains are densely grafted onto the polystyrene surface and adsorb only onto the AFM tip, the monomers are slow to desorb from the tip upon decompression and the chain elasticity reduces the force as the chains are stretched. The rate used in this experiment, corresponding to 0.001 s between measured points, was typically faster than the rates used in earlier studies, which found that relaxation of the adsorbed chains to their equilibrium configurations could take on the order of many minutes or even hours.[35]

The fact that an attractive bridging force could be measured on approach, given the high loading rate that was used here, differs from earlier results. In a study[41] where PEO had been adsorbed onto a glass surface, the lack of a detectable bridging force on compression was attributed to the high rate of approach (25 nm/s, or 0.02 s between sample points) that did not allow sufficient time for bridges to form. While this rate was much higher than in other experiments where bridging was detectable (10−60 s between sample points),[35] it is still considerably lower than that used here.

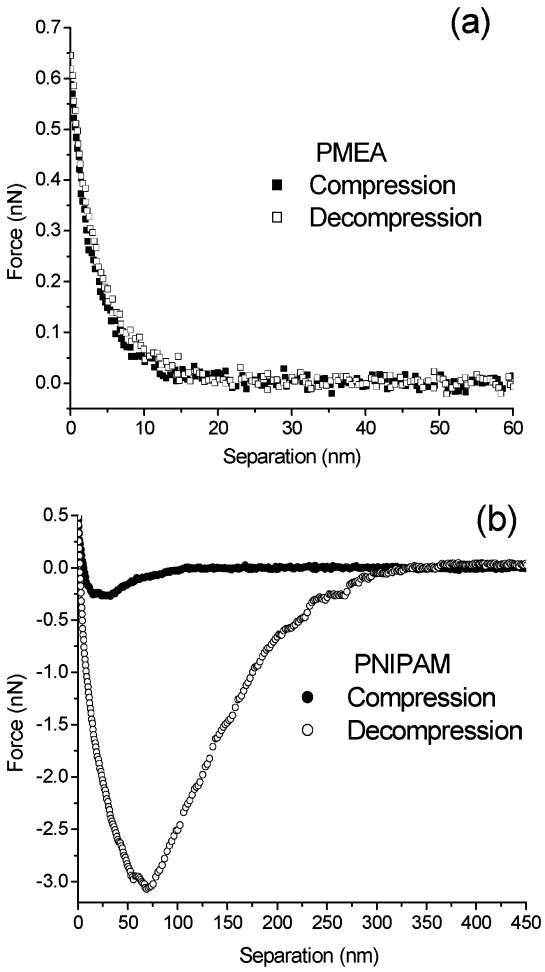

Figure 7. Compression (closed symbols) and decompression (open symbols) of brushes under conditions of equilibrium (a) PMEA ($M_n = 32\,500$, $\sigma = 0.054$ nm^2) and nonequilibium (b) PNIPAM ($M_n = 48\,000$, $\sigma = 0.037$ nm^2). Measurements were performed in 10 mM NaCl, pH 7. Curves show typical single force profiles.

Multiple compression profiles of a PNIPAM brush obtained at a given location on the sample at a rate of 1.5 μm/s were reproducible, as shown by the superposition of curves in Figure 8a. Although the relaxation times for bridged chains to return to their equilibrium structure has been shown to be long relative to the time scale of the AFM experiment, the bridged chains adhere to the tip and stretch well beyond the equilibrium thickness during the decompression cycle. The time required for a stretched chain to return to equilibrium has been calculated[16,56] to be on the order of milliseconds, which is faster than the time scale of the experiment.

Unlike the repulsive steric forces, the nonequilibrium bridging interactions depend on the rate of compression, as demonstrated in Figure 8b. Compression of the PNIPAM brush by the AFM tip in the same location as

(55) Luckham, P. F.; Klein, J. *J. Colloid Interface Sci.* **1987**, *117*, 149.

(56) Wong, J. Y.; Kuhl, T. L.; Israelachvili, J. N.; Mullah, N.; Zalipsky, S. *Science* **1997**, *275*, 820.

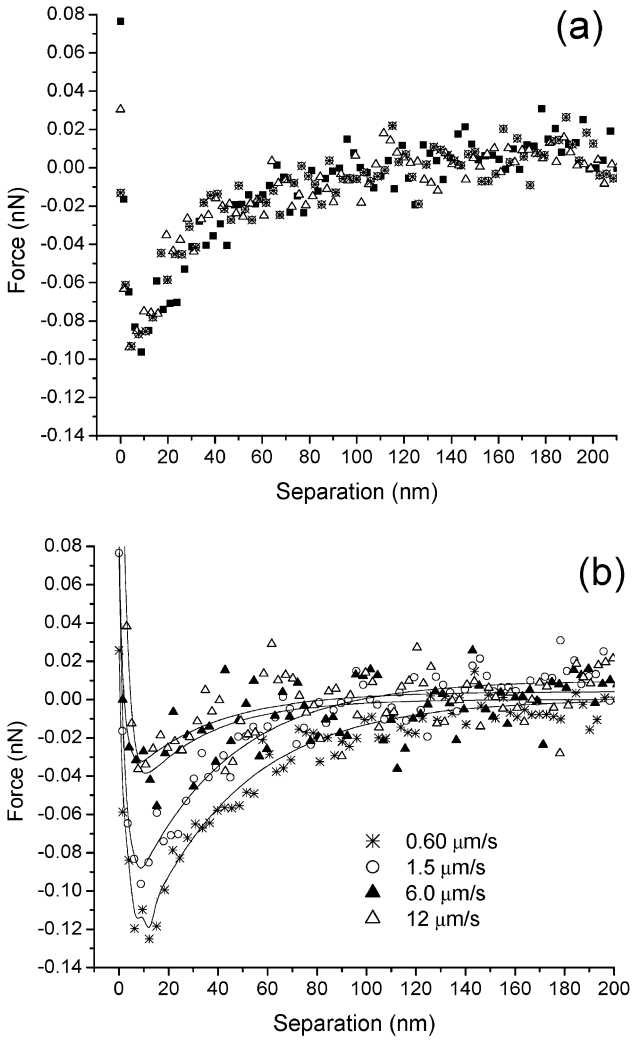

Figure 8. (a) Reproducible compression profiles of a PNIPAM brush obtained sequentially at a single sample location at a rate of 1.5 μm/s. The brush properties were $M_n = 94\,900$, PDI = 1.35, and $\sigma = 0.067$ nm^{-2}. (b) Effect of scan rate on the compression profile of the PNIPAM brush. Curves show typical single profiles. Measurements were performed at the same sample location as in panel a. Solid lines are provided to guide the eye.

that in Figure 8a showed a decrease in the magnitude of the attractive force with increasing scan rate. The results did not depend on the order in which the scans were performed. The pronounced attractive bridging force, which decreased with increasing scan rate, returned when the scan rate was reduced.

In addition to the hysteresis apparent at small separations characteristic of the slow relaxation of bridged chains, the shape of the decompression curve over the entire separation range is quite different from one in which single-chain elasticity is observed.[20,28,52] We believe that the roughly continuous decrease of the adhesion force over a large separation, larger than the contour length of the brush, reflects the polydispersity of the brush and results from the sequential detachment of chains of different lengths from the tip. The steps apparent at large separations represent the inhomogeneities in the chain lengths, particularly in the high molecular weight region where the fraction of chains of a particular length is small. The interpretation of decompression curves such as the one presented in Figure 7b is the topic of another report.[52]

Conclusion

The effect of grafting density and monomer type on the force exerted by polymer brushes in a good solvent on an AFM tip has been investigated. A long-range attractive bridging force can be observed at a sufficiently low σ, in contrast to the monotonically increasing repulsive force seen in the higher σ brushes. The density at which the bridging force could be observed was considerably larger for the PNIPAM brushes than for the PDMA or PMEA brushes. Correlation of attractive bridging forces with experimental brush properties is valuable, particularly if the grafted polymer layer is intended for stabilization. The detection of bridging at these high grafting densities, particularly in the case of PNIPAM, is somewhat unusual. One factor that may need consideration is the effect of curvature of the latex particle on the chain density away from the surface. While the fraction of polymer at the grafting surface is high, the volume fraction near the equilibrium thickness is significantly lower than if the brushes were prepared on a flat surface. Currently, further investigation into the radial effect of spherical brushes by varying the size of the latex particle is being conducted.

Acknowledgment. We thank the Canadian Institutes of Health Research, Canadian Blood Services, Natural Sciences and Engineering Research Council of Canada, and Canada Foundation for Innovation for financial support and R. Norris-Jones for help with HT measurements.

LA035843T